Electronic Supplementary Information (ESI)

A novel NIR fluorescent turn-on sensor for the detection of pyrophosphate anion in complete water system

Weihong Zhu,* Xiaomei Huang, Zhiqian Guo, Xumeng Wu, Huihui Yu and He Tian

Shanghai Key Laboratory of Functional Materials Chemistry, Key Laboratory for Advanced Materials and Institute of Fine Chemicals, East China University of Science & Technology, Shanghai 200237, P. R. China. Fax: (+86) 21-6425-2758. E-mail: whzhu@ecust.edu.cn.

Contents:

1. Experimental

1.1 General

1.2 Synthesis of (*E*)-diethyl 2,2'-((4-(2-(4-(dicyanomethylene)-4*H*-chromen-2-yl) vinyl)phenyl)azanediyl)diacetate (DCEA)

1.3 Synthesis of (*E*)-2,2'-((4-(2-(4-(dicyanomethylene)-4*H*-chromen-2-yl)vinyl) phenyl)azanediyl)diacetic acid (DCAA)

2. Absorption spectra and emission spectra of DCAA upon titration of Cu^{2+} (Fig. S1 - Fig. S3)

3. Emission spectra of DCAA-Cu^{2+} upon titration of amino acids such as Glycine and Histidine (Fig. S4)

4. Emission spectra of DCAA-Cu^{2+} upon titration of PPi (Fig. S5 - Fig. S7)

5. ^{1}H NMR, ^{13}C NMR and HRMS characterization of DCEA (Fig. S8 - Fig. S10)

6. ^{1}H NMR, ^{13}C NMR and HRMS characterization of DCAA (Fig. S11 - Fig. S13)

1. Experimental

1.1 General

All solvents were of analytical grade. Diethyl 2,2'-((4-formylphenyl)azanediyl)diacetate (2) was synthesized from diethyl 2,2'-(phenylazanediyl)diacetate (1) via Vilsmeier formylation in 60% yield (X. Meng, M. Z. Zhu, L. Liu and Q. X. Guo. *Tetrahedron Lett.*, 2006, **47**, 1559). The intermediate of 2-(2-methyl-*4H*-chromen-4-ylidene)malononitrile was prepared by the established literature procedure (G. G. Badcock, F. M. Dean, A. Robertson and W. B. Whalley, *J. Chem. Soc.*, 1950, 903). ^{1}H NMR and ^{13}C NMR in $CDCl_3$ or DMSO-d_6 were measured on a Bruker AV-400 spectrometer with tetramethylsilane (TMS) as internal standard. High Resolution Mass spectra (HRMS) were measured on a Waters LCT Premier XE spectrometer. UV-vis spectra were obtained with a Varian Cary 500 spectrophotometer (1 cm quartz cell) at 25 °C. Fluorescent spectra were recorded on a Varian Cary Eclipse fluorescence spectrophotometer (1 cm quartz cell) at 25 °C.

Cell culture: A human nasopharyngeal epidermal carcinoma cell line (KB cell) was provided by the Institute of Biochemistry and Cell Biology, SIBS, CAS (China). Cells were grown at 37°C and with 5% CO_2 in Roswell Park Memorial Institute medium (RPMI) 1640 supplemented with 10% fetal bovine serum (FBS). Cells (5×10^8 L^{-1}) were plated on 18 mm glass coverslips and allowed to adhere for 24 h. The cells were washed three times with PBS buffer, and the medium was replaced with PBS buffer before imaging.

Microscopy and imaging methods: Confocal luminescence imaging: Confocal

luminescence imaging of cells was performed with a modified Olympus FV1000 laser-scanning microscope. A 60 × oil-immersion objective lens was used. Excitation was carried out with a semiconductor laser at λ = 405 nm, and emission was collected in the range λ = 630 – 730 nm, including the maximum emission wavelength of DCAA. KB cells were incubated with a PBS solution of DCAA-Cu^{2+} (10 μM) for dye loading for 0.5 h at 37°C, then the cells were incubated with a PBS solution of PPi (30 μM) for 0.5 h at 37°C. The stained cells were washed three times with PBS buffer. Then the treated cells were imaged by fluorescence microscopy.

1.2 Synthesis of (*E*)-diethyl 2 ,2'-((4-(2-(4-(dicyanomethylene)-4*H*-chromen-2-yl) vinyl)phenyl)azanediyl)diacetate (DCEA)

2-(2-methyl-*4H*-chromen-4-ylidene)malononitrile (0.62 g, 3.0 mmol) and diethyl 2,2'-((4-formylphenyl)azanediyl)diacetate (1.09 g, 3.7 mmol) were dissolved in toluene (40 ml) with piperidine (0.5 ml) and acetic acid (0.5 ml) under argon protection at room temperature. Then the mixture was refluxed and stirred for 8 h. The solvent was evaporated in vacuo, and the crude solid was purified by column chromatography on silica gel eluting with petroleum ether/ethyl acetate (5/1, v/v) to afford a red solid in 48% yield. ^{1}H NMR (400 MHz, $CDCl_3$): δ 8.92 (d, J = 8.4 Hz, 1H, phenyl-H)，7.71 (t, J = 6.8 Hz, 1H, phenyl-H), 7.56 (d, J = 15.6 Hz, 1H, alkene-H), 7.54 (d, J = 3.2 Hz, 1H, phenyl-H), 7.45 (m, 3H, phenyl-H), 6.81 (s, 1H, pyran-H), 6.65 (d, J = 8.8 Hz, 2H, phenyl-H), 6.62 (d, J = 15.6 Hz, 1H, alkene-H), 4.25 (q, 4H, -C$H_2$$CH_3$), 4.19 (s, 4H, -NC$H_2$-), 1.30 (t, J = 6.8 Hz, 6H, -CH_2CH_3). ^{13}C NMR (100 MHz, $CDCl_3$): δ 170.09, 158.48, 152.88, 152.37, 149.83, 139.18, 134.36, 129.88,

125.78, 125.74, 124.73, 118.51, 117.94, 117.24, 116.17, 114.55, 112.60, 105.78, 61.50, 61.07, 53.37, 14.25. HRMS (ESI): calcd for $C_{28}H_{24}N_3O_5$ $[M - H]^-$ 482.1716, found 482.1715.

1.3 Synthesis of (*E*)-2,2'-((4-(2-(4-(dicyanomethylene)-4*H*-chromen-2-yl)vinyl) phenyl)azanediyl)diacetic acid (DCAA)

(*E*)-diethyl 2,2'-((4-(2-(4-(dicyanomethylene)-4*H*-chromen-2-yl)vinyl)phenyl)azanediyl)diacetate (0.15 g, 0.31 mmol) was dissolved in a 1:1 THF/CH_3OH mixture (30 ml), and treated with 10 equiv. of lithium hydroxide (0.13 g, 3.1 mol). The mixture was reacted at room temperature for 5 min, at which time TLC analysis showed complete consumption of starting material. The reaction was evaporated to dryness, then the crude product was purified by silica gel column chromatography (CH_2Cl_2/MeOH = 15:1 v/v) to give DCAA as a red solid (0.13 g, 48% yield). ^{1}H NMR (400 MHz, DMSO-d_6): δ 8.72 (d, J = 8.0 Hz, 1H, phenyl-H), 7.89 (t, J = 7.6 Hz, 1H, phenyl-H), 7.80 (d, J = 8.3 Hz, 1H, phenyl-H), 7.69 (d, J = 16.0 Hz, 1H, alkene-H)，7.59 (m, 3H, phenyl-H), 7.20 (d, J = 16.0 Hz, 1H, alkene-H), 6.91 (s, 1H, pyran-H), 6.52 (d, J = 8.1 Hz, 2H, phenyl-H), 4.05 (s, 4H, -NCH_2-). ^{13}C NMR (100 MHz, DMSO-d_6): δ 173.40, 159.35, 152.60, 152.01, 139.89, 135.02, 130.18, 125.86, 124.47, 118.93, 117.13, 116.29, 113.78, 111.44, 105.10, 79.27, 78.94, 78.61. HRMS (ESI): calcd for $C_{24}H_{16}N_3O_5$ $[M - 2Li + H]^-$ 426.1090, found 426.1089.

2 Absorption spectra and emission spectra of DCAA upon titration of Cu^{2+}

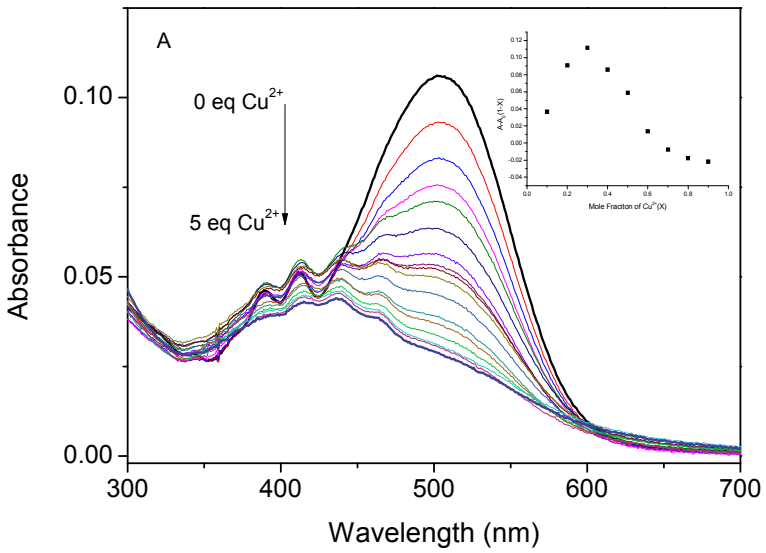

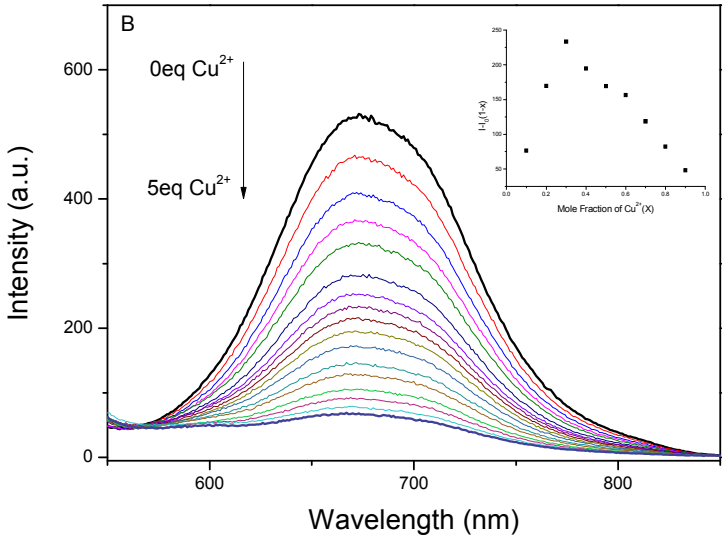

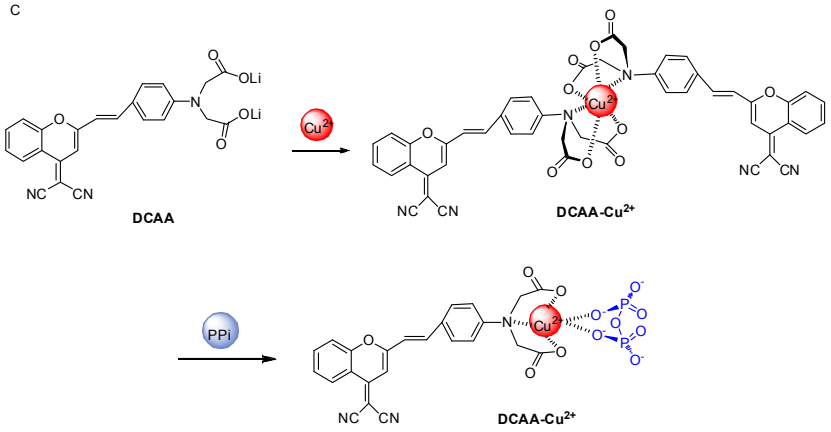

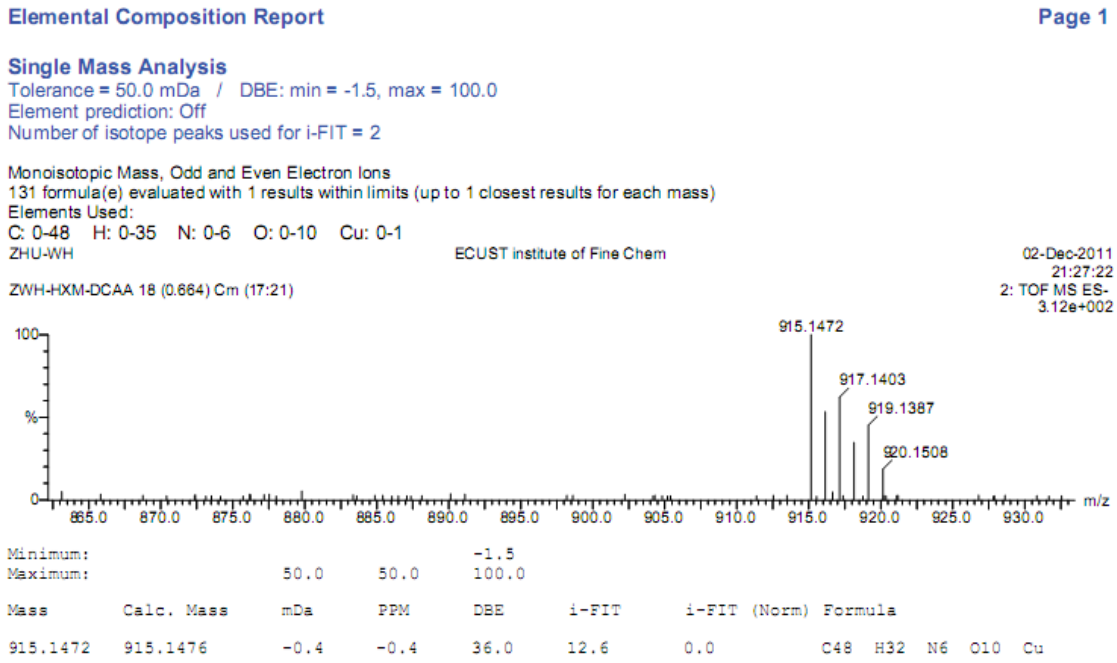

Fig. S1 Absorption spectra (A) and emission spectra (B) of **DCAA** (10 μM) with excitation wavelength at 500 nm in MOPS (10 mM, pH = 7.0) buffer solution of upon titration of Cu^{2+} (0, 0.2, 0.4, 0.6, 0.8, 1.0, 1.2, 1.4, 1.5, 1.6, 1.8, 2.0, 3.0, 5.0 equiv.). Inset: the job plots with both absorption and fluorescence titrations exhibited a maximum at about 0.33 mol fractions, indicating that **DCAA** forms a 2:1 complex with Cu^{2+}. (C) The possible sensing mechanism of **DCAA-Cu** and **PPi**, and the high resolution mass spectra (HRMS) of **DCAA-Cu**. Note, the mass peak for **DCAA-Cu**$^{2+}$ at *m/z* 915.1472 corresponding to $[C_{48}H_{32}N_6O_{10}Cu]^-$ (= [2DCAA + Cu^{2+} + 2H]$^-$ calculated as 915.1476) gives strong evidence that **DCAA** forms a 2:1 complex with Cu^{2+}.

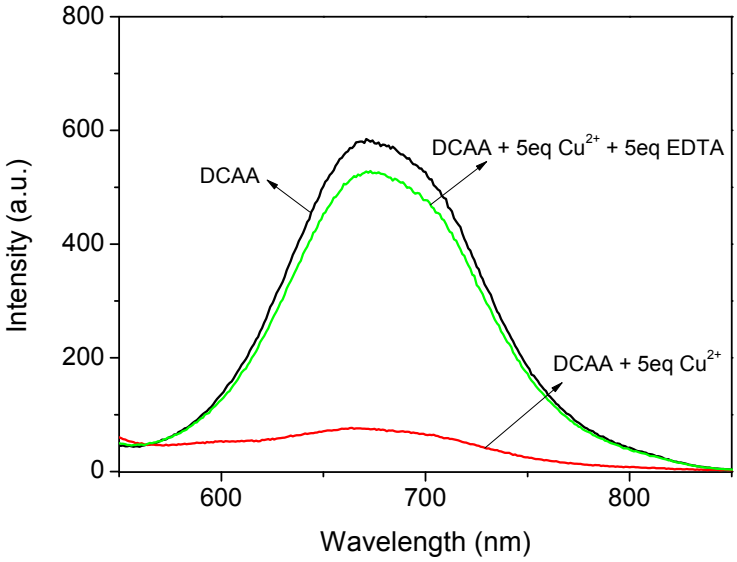

Fig. S2 Fluorescence spectra of **DCAA** in the absence and presence of Cu^{2+} and the addition of **EDTA**.

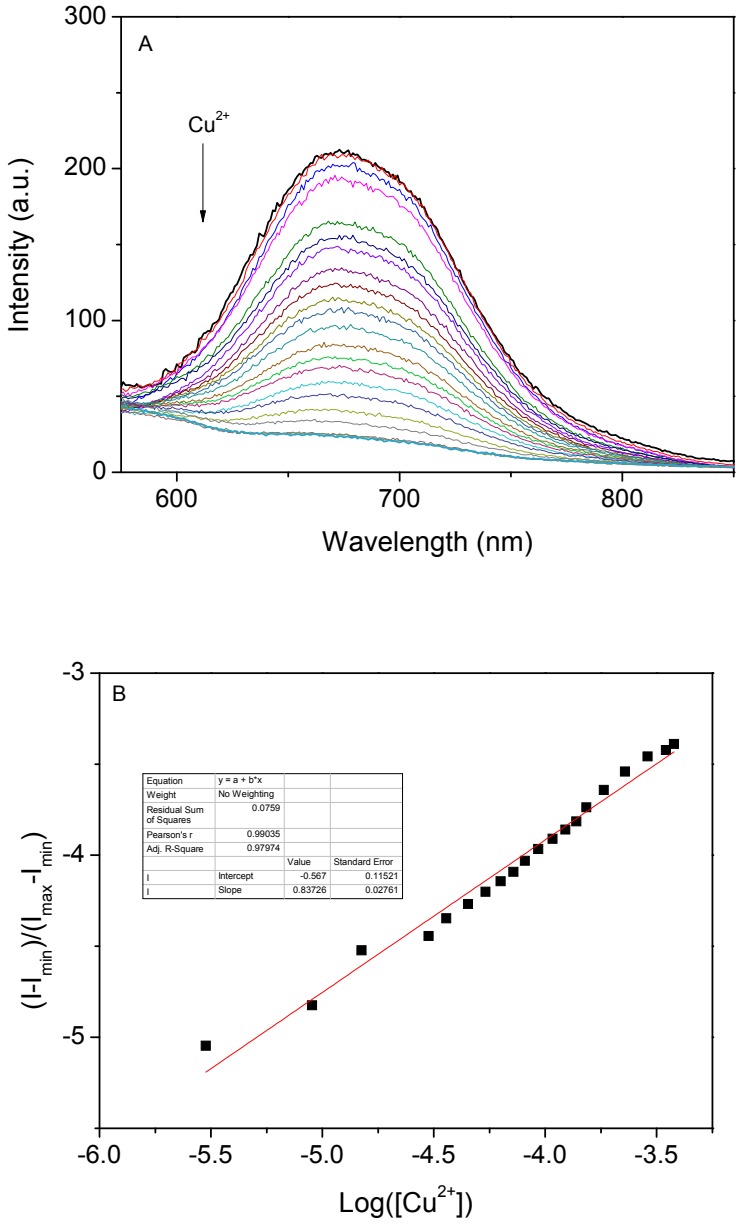

Fig. S3 A) Fluorescence changes during the titration of **DCAA** (3 μM) with Cu^{2+} (0-10 equiv.) in MOPS (10 mM, pH = 7.0) buffer solution; B) A plot of (I - I_{min}) / (I_{max} - I_{min}) *vs* Log([Cu^{2+}]), the calculated detection limit of **DCAA** is 1.26×10^{-6} M.

3 Emission spectra of DCAA-Cu^{2+} upon titration of amino acids such as Glycine and Histidine

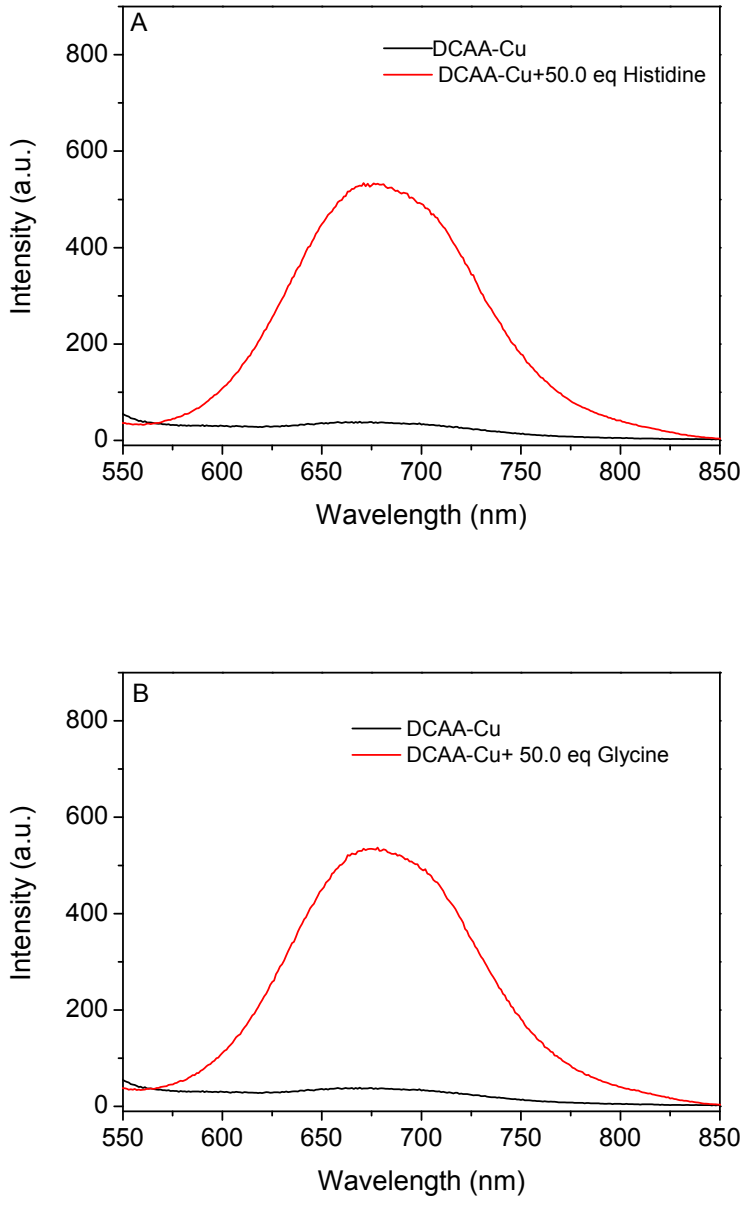

Fig. S4 Emission change of **DCAA-Cu^{2+}** (10 μM) in an aqueous solution buffered with MOPS (10 mM, pH = 7.0) upon titration with 50.0 equiv. of Histidine and Glycine.

4 Emission spectra of DCAA-Cu^{2+} upon titration of PPi

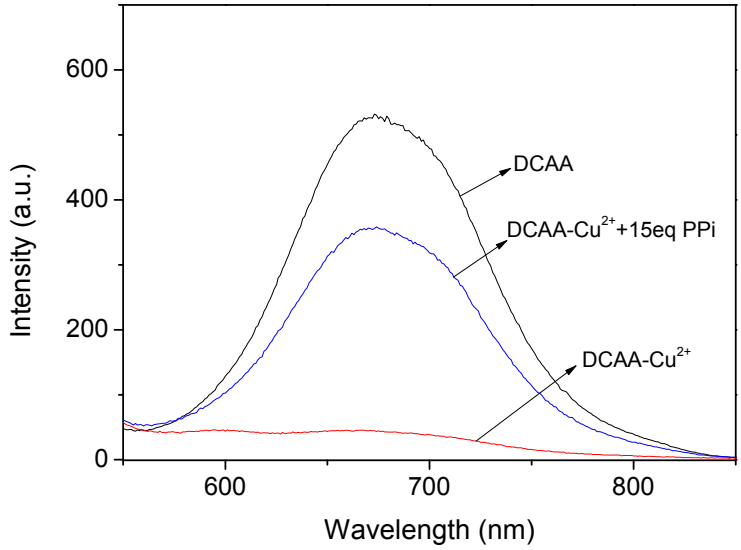

Fig. S5 Emission change of **DCAA-Cu^{2+}** (10 μM) in an aqueous solution buffered with MOPS (10 mM, pH = 7.0) upon titration with 15 equiv. of PPi.

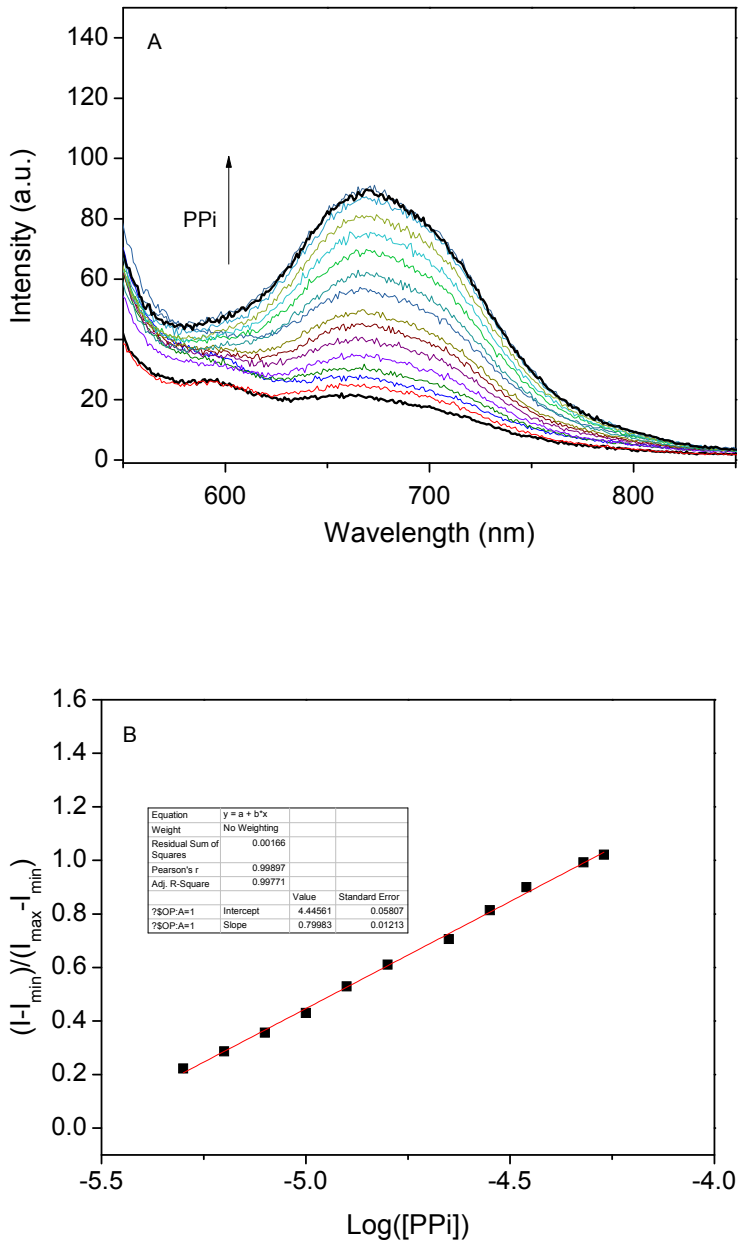

Fig. S6 A) Fluorescence changes during the titration of **DCAA-Cu^{2+}** (3 μM) with PPi (0-20 equiv.) in MOPS (10 mM, pH = 7.0) buffer solution; B) A plot of (I - I_{min}) / (I_{max} - I_{min}) *vs* Log([PPi]), the calculated detection limit of **DCAA-Cu^{2+}** is 2.02 × 10^{-6} M.

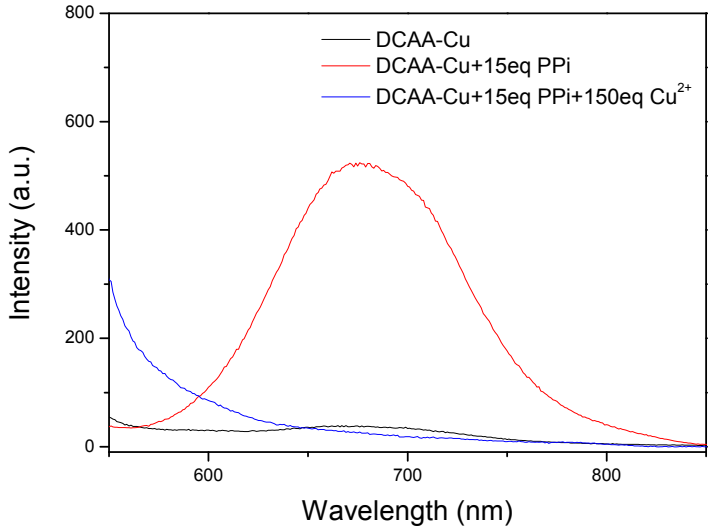

Fig. S7 Emission change of **DCAA-Cu^{2+}** (10 μM) in an aqueous solution buffered with MOPS (10 mM, pH = 7.0) upon titration with 15 equiv. of PPi and 150 equiv. of Cu^{2+}. Note: The chemosensor detection of PPi is reversible. When PPi was added gradually to the solution of **DCAA-Cu^{2+}**, the fluorescence intensity was obviously enhanced and stabilized upon addition of 15 equiv. of PPi. Reversibly, when adding exceeded Cu^{2+} to the solution above, the fluorescence intensity was quenched gradually and it's quenched completely in 150 equiv. of Cu^{2+}.

5 ^{1}H NMR, ^{13}C NMR and HRMS characterization of DCEA

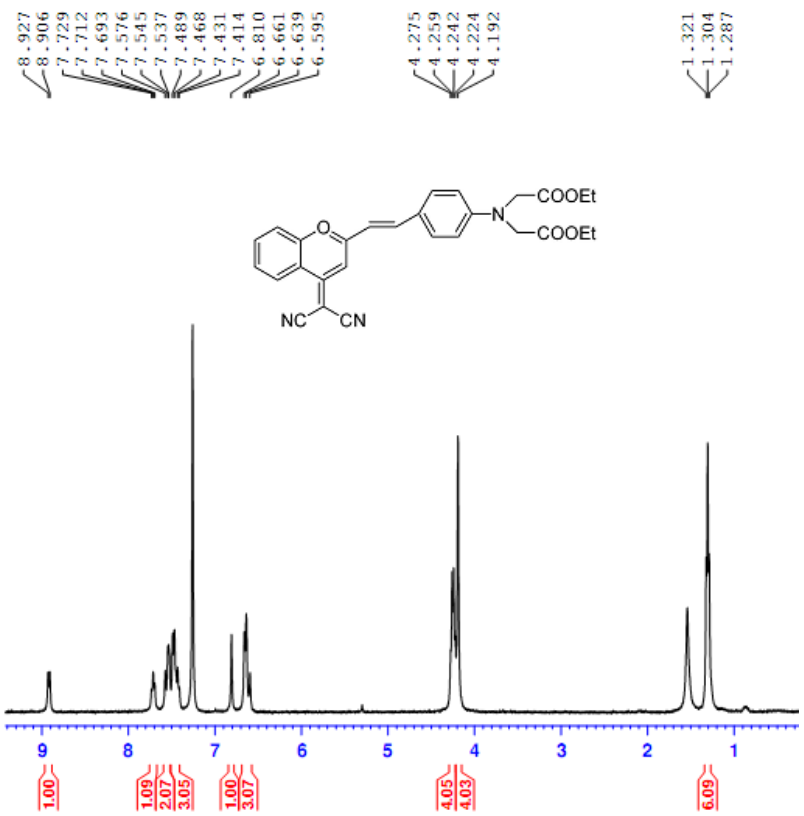

Fig. S8 ^{1}H NMR spectra of **DCEA** in $CDCl_3$

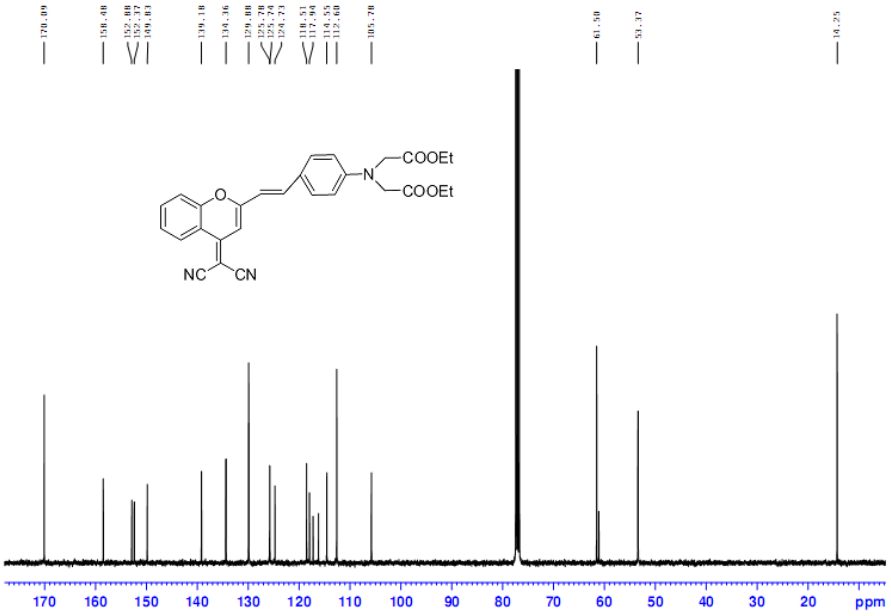

Fig. S9 ^{13}C NMR spectra of **DCEA** in $CDCl_3$ (100 MHz)

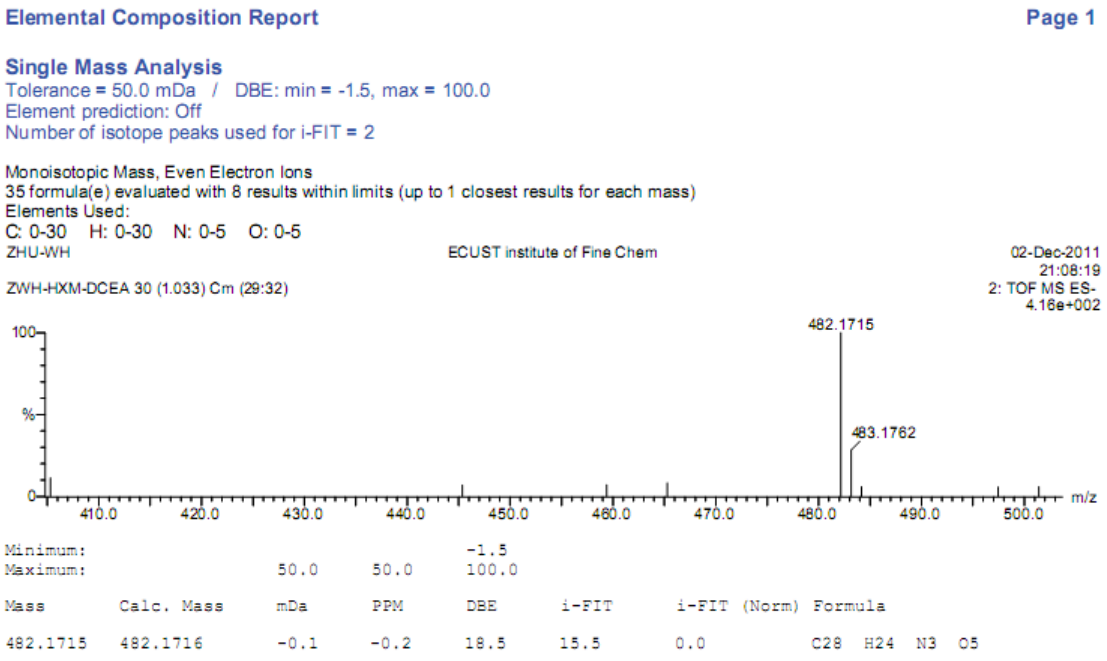

Fig. S10 High resolution mass spectra (HRMS) of **DCEA**

6 ^{1}H NMR, ^{13}C NMR and HRMS characterization of DCAA

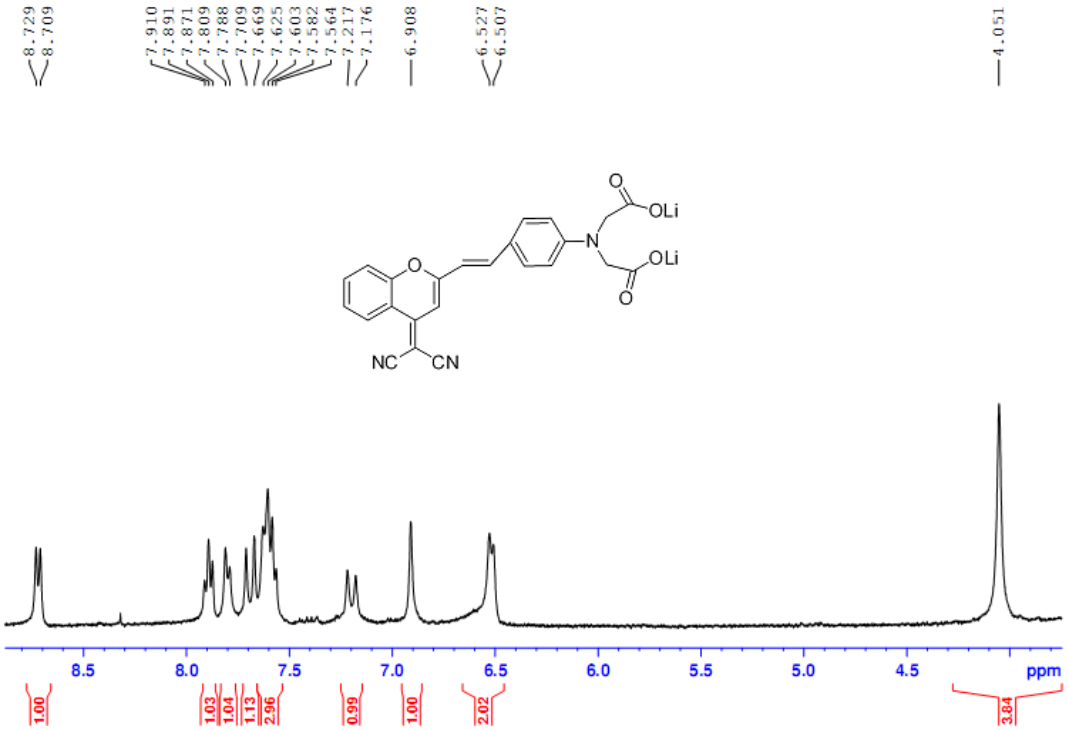

Fig. S11 ^{1}H NMR spectra of **DCAA** in DMSO-d_6

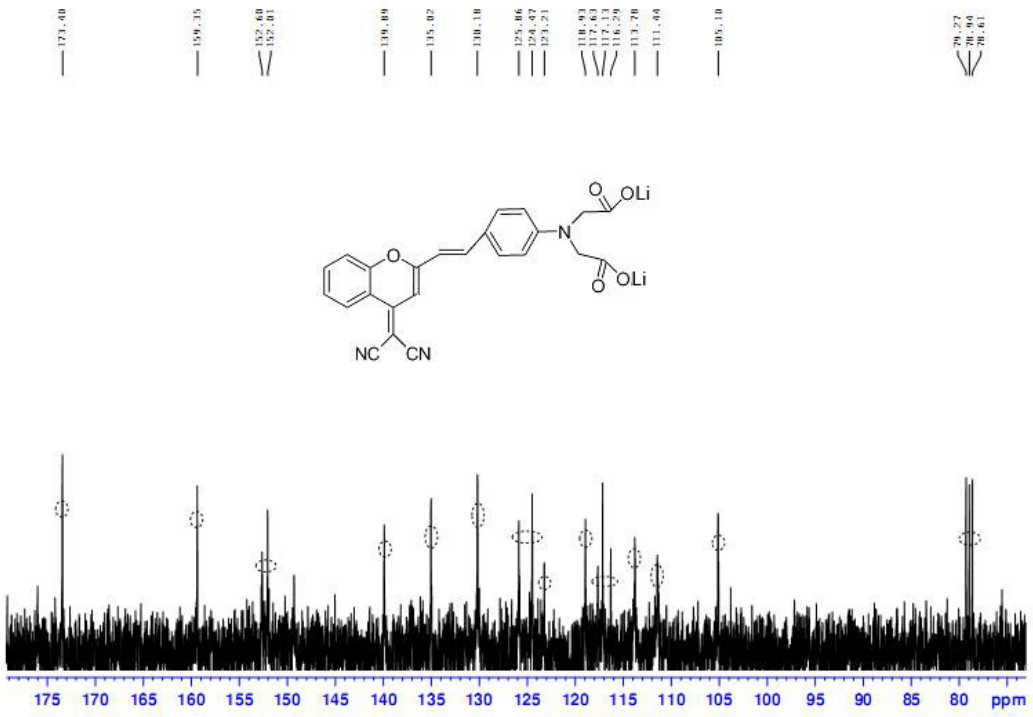

Fig. S12 ^{13}C NMR spectra of **DCAA** in DMSO-d_6 (100 MHz)

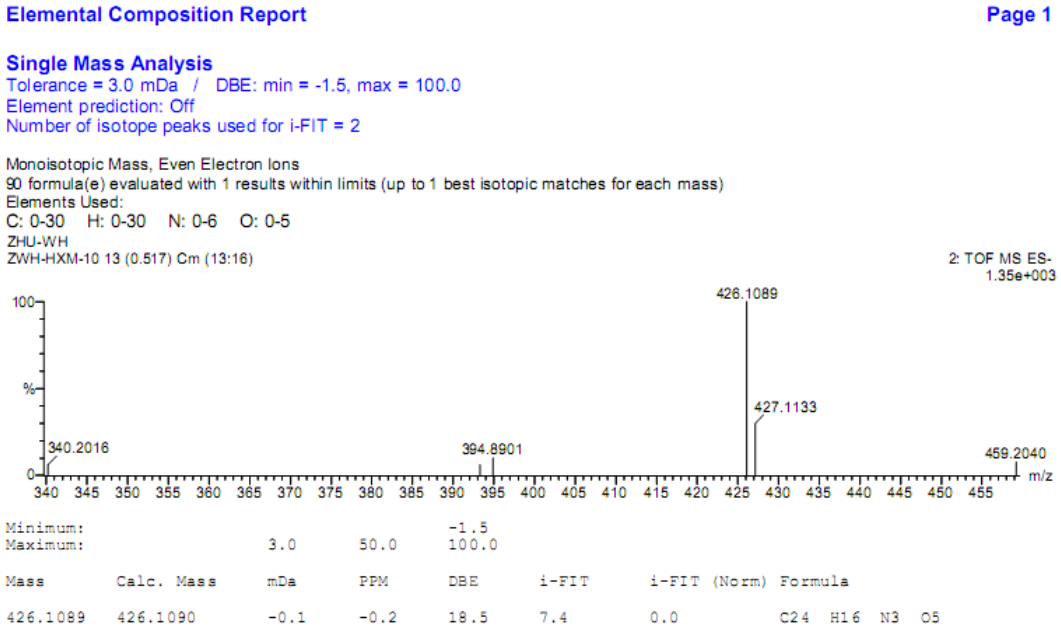

Fig. S13 High resolution mass spectra (HRMS) of **DCAA**